Surface Biophysics of the Surface Monolayer Theory Is Incompatible with Regional Lung Function

Emile M. Scarpelli* and Alan J. Mautone‡

*Perinatology Center, Cornell University Medical College, New York, New York; ‡Departments of Anesthesiology, Pediatrics, and Physiology, UMD-New Jersey Medical School, Newark, New Jersey

ABSTRACT The surface monolayer theory of Clements was tested on open surface films of calf lung surfactant extract in a leak-free vertical film surface balance in which alveolar area (A) changes in each lung zone were simulated in accordance with the theory. We found that: 1) physiologically necessary low surface tension (γ), <4 dyn/cm, was sustained only by continuous film compression ("expiration"); 2) compression from A equivalent to total lung capacity to functional residual capacity produced fleeting γ reduction in all zones and quick reversal to high γ with A changes that simulated tidal volume (V_T) breathing at both 14 (adult) and 40 (neonatal) cpm; 3) phase differences between γ and A axes of V_T loops that indicate mixed surface film composition may be attributable to film inertia and viscoelasticity; 4) estimated alveolar retraction pressure due to γ ($P\gamma$) exceeds "net" transpulmonary pressure, i.e., favors alveolar collapse, under virtually all conditions of the theory in all zones; 5) return to transient, fleeting low γ in successive V_T cycles was determined by the inherent difference in compression and decompression rates, which results in exhaustion of available A in very few cycles; 6) the "sigh", which restores stable low γ according to the theory, actually produced unstable high γ during virtually all phases of the maneuver. In contrast, closed bubble films of the surfactant were structurally stable and produce stable near 0 γ and $P\gamma$.

INTRODUCTION

The physiological significance of stable virtually 0 surface tension (γ) as an "antiedema" factor was first proposed by Pattle (1955, 1958) in his reports of the discovery of lung surfactant. He showed that films of bubbles expressed from normal lungs (a laboratory artifact according to Pattle) possessed these characteristics. He suggested that alveolar open films in situ provide the material for bubble film formation in vitro and that both films share the same characteristics. This concept of virtually 0 γ in vivo was reinforced (Scarpelli, 1971), and a new concept was offered (Scarpelli, 1978) that surfactant closed bubble films are formed naturally in vivo where they establish virtually 0 γ while also providing mechanical infrastructural support against alveolar collapse (Scarpelli, et al., 1984).

In contrast, the surface monolayer theory of open alveolar films, as first introduced by Clements (1962), held that alveolar γ was relatively high (<10–15 dyn/cm), variable (more or less following the γ-surface area (A) isotherms of surfactant films during compression-decompression in a surface balance), and unstable when the film is maximally compressed (Clements, 1962; King and Clements, 1972a,b). This theory has been modified and summarized as follows (Goerke and Clements, 1986). A film highly enriched in dipalmitoylphosphatidylcholine (DPPC) is formed at the interface between the alveolar gas phase and a liquid hypophase covering the epithelium. The open film, which tends to spread away from the periphery, is continuous among alveoli, as shown in Fig. 1 (Hawgood and Clements, 1990). According to the theory (Goerke and Clements, 1986), formation and function of the monolayer film are governed by expansion and contraction of alveolar A during normal breathing. When the monolayer is significantly expanded (decompressed), as during inspiration to total lung capacity (TLC), surfactant is adsorbed from hypophase to bare regions of the interface, rapidly spreading over the surface and forming regions especially rich in DPPC. When the surface is contracted (compressed) during expiration to functional residual capacity (FRC), regions of DPPC-poor films are "squeezed out", leaving a nearly pure DPPC monolayer that resists rapid collapse and prevents adsorption of new material to the interface during subsequent tidal volume (V_T) breathing. These film transformations explain surfactant function during normal breathing as follows. According to the theory, γ is reduced to near 0 dyn/cm during expiration from TLC to FRC and this low γ is sustained. Periodically, the process (inspiration to TLC, expiration to FRC) is repeated, the open film is restored, and near 0 γ is reestablished. The conditions of the surface monolayer theory have not been tested directly.

To test the theory, we considered the broad inhomogeneity of alveolar A, and the differential effect of respiratory movements on A change as functions of alveolar location. When the upright adult lung is at FRC, its upper region (zone 1) operates at or near TLC for that region, whereas the middle region (zone 2) operates at or near its FRC and the lower region (zone 3) operates at or near its residual volume (RV). Given that alveoli of all zones follow the same pressure-volume (P-V) curves, V and A characteristics of each zone during breathing movements are predictable (Gil et al., 1979; Hoffman and Heymann, 1990; Mercer et al., 1987; Millic-Emili, 1974, 1986).

Received for publication 29 November 1993 and in final form 7 June 1994.

Address reprint requests to Alan J. Mautone, PhD, Department of Anesthesiology, UMD-New Jersey Medical School, 185 South Orange Avenue, Newark, New Jersey 07103. Tel.: (201) 982–7669; Fax: (201) 982–4172; E-mail: mautone@njmsa.umdnj.edu.

0006-3495/94/09/1080/10 $2.00

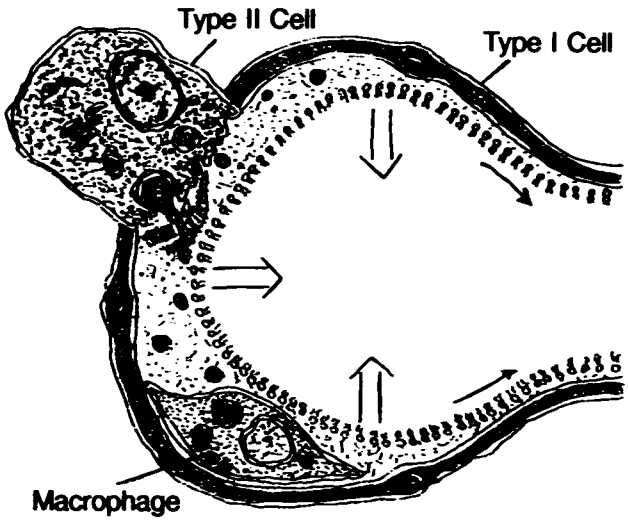

FIGURE 1 Monolayer film of alveolar surfactants ( ) at the interface between alveolar gas and the liquid hypophase that covers alveolar epithelial cells and extracellular macrophage. According to the surface monolayer theory of surfactant function, the hypophase and monolayer film ("open" film) are continuous among alveoli. The two thin arrows indicate the direction in which the surfactants of the film tend to move, namely, out of the alveoli. Diagram was redrawn after Hawgood and Clements (1990). The three broad arrows were added to show the direction of the retractive ("collapse") pressure that would be generated by the surface tension ($P\gamma$) of the monolayer film.

We used a leak-free surface balance (Boyle and Mautone, 1982; Mautone et al., 1988) to simulate alveolar A changes in surface monolayer films that are relevant to the surface monolayer theory, namely, A changes between TLC and FRC, and during V_T breathing, according to alveolar position in the lung zones. The substrate was calf lung surfactant extract (CLSE), a preparation successfully used in treatment of respiratory distress syndrome in immature fetal animal models (Cummings et al., 1992) as well as in preterm babies (Shapiro et al., 1985), which is rich in DPPC and forms an open film at the air-liquid interface in the surface balance. Experiments were designed to test point by point each of the assumptions and conditions of the surface monolayer theory as given by the authors of the theory (Goerke and Clements, 1986) with regard to surfactant function in vivo.

MATERIALS AND METHODS

Surface active material

CLSE (generously supplied by Dr. Bruce Holm, Children's Hospital of Buffalo, Buffalo, NY) was prepared according to the method used by Hall et al. (1992). Briefly, fresh calf lungs were lavaged with normal saline solution and the lavagate was centrifuged at 300 × g for 10 min to remove cells and debris. The supernatant was centrifuged at 12,000 × g for 1 h, and a hydrophobic extract was obtained from the pellet according to the method of Bligh and Dyer (1959). The extract was dried under nitrogen and stored at −20°C. On the day of the study, the extract was suspended in normal saline solution at a concentration of 12 mg total phospholipid/ml. Composition was 90–94% phospholipid of which ≈80% was phosphatidylcholine (80% disaturated species), 6% phosphatidylglycerol, 3% phosphatidylethanolamine, 5% phosphatidyl inositol/serine, 2% sphingomyelin, and <1% lysolecithin; 4% neutral lipids; and 1% protein (including surfactant-associated proteins SP-B and SP-C). The CLSE has been reported to have normal surfactant function in vitro (Cummings et al., 1992; Hall et al., 1992; Egan et al., 1984).

Surface balance

To eliminate surface film leakage while retaining the accuracy of the conventional Langmuir-Wilhelmy surface balance, we used a vertical film surface balance (Boyle and Mautone, 1982). Surface tension-surface area (γ-A) isotherms of open, planar surface films were recorded at 37°C, and air phase over the film was saturated with water vapor at this temperature. The apparatus and method have been described (Boyle and Mautone, 1982; Mautone et al., 1988). Briefly, the balance consists of a fine-mesh stainless steel screen that is moved vertically into and out of the hypophase of the test material. The surface is at minimum area (A_{min}; 31.7 cm^2) when the screen is submerged in the hypophase, bulk CLSE in our study. As the screen is lifted vertically, film A increases while film continuity is maintained; A_{max} may be selected by the experimenter. In our study, A_{max} or 100% A was 142.6 cm^2. The amplitude of each compression-decompression cycle may be varied between 100% A and the limiting 22% A, A_{min}. Surface tension is measured with an electrobalance (Nima 9000, Nima Technology, Coventry, UK) from a wettable platinum plate with negligible contact angle. The Teflon reservoir of the balance holds 40 ml of test material.

Both γ and A were recorded online to a microprocessor using a Metrabyte DAS-8 A/D converter and software (Labtech Notebook, Laboratory Technologies Corp., Wilmington, MA) so that data was viewed onscreen during collection at a sampling rate of 30 Hz. Evaluation of frequency response characteristics of the system from platinum plate through recording of data showed that the time constant was 0.164 s, with a phase lag of −0.9° at 6 cpm, −2.2° at 14 cpm, and −6.2° at 40 cpm. Damping was not significant at cycling rates below 60 cpm.

Estimation of regional surface area

Lung V was estimated from P-V curves presented by Milic-Emili (1974, 1986). With TLC as 100% V, FRC is ≈40% V, RV is ≈20% V, and minimal volume (V_{min}) is ≈10% V (Table 1). When the adult lung in the upright position is at TLC, all zones are at their respective TLC; however, when the lung is at FRC, the approximate midposition of each zone, respectively, is at 75% V (zone 1), 40% V (zone 2) and 20% V (zone 3) (Table 2). When the lung is at FRC, the V change per breath during normal V_T breathing is ≈3.5% V for zone 1, ≈10% V for zone 2, and ≈11% V for zone 3 (Table 2). Because of its diminutive size and usual recumbent position, the neonatal lung operates primarily under zone 3 conditions (Hoffman and Heymann, 1990).

Alveolar V and A correlations have been established from three-dimensional reconstructions of rat alveoli by Mercer et al. (1987) and from morphometric analysis of rabbit alveoli by Gil et al. (1979). Given that all lung regions have the same P-V characteristics, we could estimate proportional alveolar A for each region from the same data (Table 2). With the lung at TLC, each region is at ≈100% A; with the lung at FRC, zone 1 is at ≈85%

TABLE 1 Derived proportional volumes and corresponding alveolar surface areas

Status	Volume (%)	Alveolar surface area (%)
TLC	100	100
FRC	40	54
RV	20	36
V_{min}	10	22

Proportional volumes derived from Milic-Emili, (1974, 1986) and corresponding alveolar surface areas, extrapolated from Mercer et al. (1987) and Gil et al. (1979) at total lung capacity (TLC), functional residual capacity (FRC), residual volume (RV) and minimal volume (V_{min}).

TABLE 2 Proportional volumes and corresponding alveolar surface areas for approximate midpositions of each region of the lung

	Regional volumes and areas (%)					
	Zone 1		Zone 2		Zone 3	
Total lung volume	Volume	Area	Volume	Area	Volume	Area
TLC	100	100	100	100	100	100
FRC	75	85	40	54	20	36
V_T from FRC	3.5	4	10	9	11	12

Proportional volumes and corresponding alveolar surface areas for the approximate mid-positions of each region of the lung when total lung volume is at TLC and FRC and during tidal breathing excursions when the lung is at FRC. Volume data derived from Milic-Emili (1974, 1986); corresponding alveolar surface areas extrapolated from data of Mercer et al. (1987) and Gil et al. (1979).

A; zone 2, ≈54% *A*; and zone 3, ≈36% *A*; during V_T breathing from FRC, cyclic *A* changes per breath were estimated as ≈4% *A* (zone 1), ≈9% *A* (zone 2), and ≈12% *A* (zone 3) for the midzone positions.

Standard γ-*A* isotherms and simulation of the surface monolayer theory

Forty milliliters of CLSE at 37°C was placed in the reservoir of the surface balance. The air phase was kept at 100% relative humidity. The hypophase was stirred continuously with a magnetic stirrer, and an uninterrupted sequence of compression-decompression cycles was started after 5 min. First, the surface film was cycled between 100% *A* and 22% *A* at 6 cpm until γ-*A* isotherms were reproduced in three consecutive cycles. This is a standard procedure for assessing "normal" surfactant function (Clements, 1962; Scarpelli, 1988). The film was then compressed from 100% *A* to one of the three *A* that represent regional *A* when the lung is at FRC (Table 2). This maneuver simulated expiration to FRC after inspiration to TLC. Cycle amplitude and rate were then changed without interruption to simulate V_T breathing in one of the three zones at a rate of either 14 cpm (adult frequency) or 40 cpm (neonatal frequency) (Table 2). Simulated V_T breathing was sustained for 2–5 min. In two trials at 14 and 40 cpm under zone 2 conditions, *A* at end-compression was reduced by ≈1% *A* in each of the first several V_T cycles while retaining ≈9% *A* change/cycle. This simulated "gradual" reduction of alveolar *A* during V_T breathing as postulated in the surface monolayer theory (Goerke and Clements, 1986). Cycling between 100% *A* and 22% *A* at 6 cpm was then resumed without interruption for comparison with the initial standard cycles. Altogether, four samples of CLSE were tested in each of the six protocols; total time for each protocol was 3.5–6.5 min.

Under conditions of zero airflow in the lung, the two major components of total transpulmonary pressure (P_{tp}) are pressures required to balance tissue force (P_{tis}) and γ($P\gamma$). We calculated "net P_{tp}" as total P_{tp} minus P_{tis}. Net P_{tp}, therefore, is pressure available to balance $P\gamma$. $P\gamma$ was calculated from the Laplace equation, $P\gamma = (2)\,(9.8)\,(\gamma)/(r)$, where (2) and (9.8) are geometric and unit conversion constants, respectively, γ is dyn/cm, and r is in μm. Alveolar radius at full inflation was taken as 125 μm for adults (Weibel, 1963) and 25 μm for neonates (Engel, 1962). The data of Mercer et al. (1987) were used to approximate proportional reduction of alveolar radius at FRC (78 μm, adult; 19 μm, neonate) and during V_T breathing (102 μm, adult; 22 μm, neonate). Total P_{tp} was taken from air deflation curves and P_{tis} both from liquid deflation curves and from curves based on measurements of alveolar wall length tension characteristics as summarized by Hoppin and Hildebrandt (1977). The two methods for estimating P_{tis} differ only at high lung *V*.

Additional experiments and related phenomena

"Normal" γ_{min} at A_{min} was taken as <4 dyn/cm. Given that the conventional *A* limits of standard γ-*A* curves, 100% *A* and 20–30% *A*, simulate lung *V* change between TLC and V_{min}, a maneuver that cannot be effected when the chest wall is intact, we also studied the effect of changing *A* limits while retaining the γ_{min} criterion. In four separate experiments, after reproducible γ-*A* isotherms were obtained by the standard method, A_{min} was increased stepwise in successive cycles, whereas A_{max} was unchanged: A_{max}–A_{min} limits were thereby decreased from 100% *A*–22% *A* to 100% *A*–50% *A*. After decompression from ≈50% *A*, the surface was compressed without interrupting cycle rate from ≈80% *A* instead of 100% *A*.

In an additional set of four experiments, three trials each, we simulated the conditions of a "sigh", i.e., inspiration from V_T to TLC after a period of V_T breathing, followed by expiration to FRC and resumption of V_T breathing. Standard cycles were followed in uninterrupted sequence by V_T cycling at 8–12% *A* for 2 min, decompression to 100% *A*, compression to 45–50% *A*, and repeat V_T cycling. The role of the "sigh" or "large breath" according to the surface monolayer theory is to restore the surface film and lung *V* (Goerke and Clements, 1986).

RESULTS

Standard γ-*A* isotherms

The range of γ_{min} for all standard isotherms was 1.5–3.0 dyn/cm at 22% *A*; γ_{max} was 32–35 dyn/cm at 100% *A* (Fig. 2, *point 1*). Surface tension fell at a mean rate ($d\gamma/dt$) of 9–12 dyn/cm/s during compression from 100% *A* to the knee in the compression isotherm at 45–60% *A* (Fig. 2, *arrow 2*); continued compression to 22% *A* (Fig. 2, *arrow 3*) had little additional effect on γ reduction. Surface tension increased at a mean rate of 18–24 dyn/cm/s during decompression from 22% *A* to the knee in the isotherm at 42–50% *A* (Fig. 2, *arrow 4*). The rate, $d\gamma/dt$, during decompression was 1.6–2.0 times greater than $d\gamma/dt$ during compression. Continued decompression to 100% *A* had little effect on γ (Fig. 2, *arrow 5*).

Extrapolations from the standard γ-*A* curves to alveolar *A* in the upright lung at FRC are noted in Fig. 2, where the approximate midposition of each zone is indicated by a vertical broken line. In contrast with the differences in proportional alveolar *A* among zones when the lung is at FRC, all zones are at ≈100% *A* when the lung is at TLC (Fig. 2, *point 1*). When lung *V* is reduced from TLC to FRC, the *A* of each zone returns, respectively, to the *A* designated by the vertical broken lines. If alveolar γ falls during deflation from TLC to FRC, as predicted in the surface monolayer theory, alveolar γ would decrease in each zone to the point where the

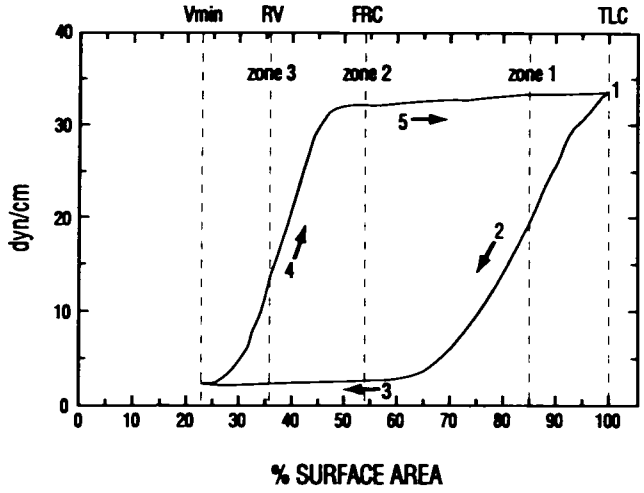

FIGURE 2 Standard surface tension-surface area (γ-A) diagram of CLSE during compression (*arrows 2 and 3*) and decompression (*arrows 4 and 5*) between 100 and 22% surface area (A). Lung volume equivalents are TLC at 100% alveolar A (*1*); FRC at ≈54% A; RV at ≈36% A; and V_{min} at ≈22% A. Vertical broken lines show the approximate midposition of the lung zones on the A axis.

compression isotherm intersects the vertical broken line for that zone. During compression from TLC to FRC equivalent, we found that the range of γ was 19–24 dyn/cm at the midposition of zone 1 and <4 dyn/cm at the midpositions of zones 2 and 3 (Table 3).

Simulation of the surface monolayer theory

Surface tension-surface area loops for V_T cycles at 14 and 40 cpm, superimposed on the standard γ-A diagram, are shown in Fig. 3, A and B, respectively, including the first V_T γ-A loop and a subsequent reproducible loop for each zone. In all trials, including those in which A at end-compression had been reduced "gradually" in successive cycles, γ increased immediately as V_T cycling began from 19–24 dyn/cm in zone 1 and from <4 dyn/cm in zones 2 and 3, and continued to increase until succeeding V_T γ-A loops were reproducible after 3 to 12 cycles. A summary of changes in each zone is given in Table 3. The γ limits or cycle amplitude, i.e., γ_{min} to γ_{max}, for reproducible V_T loops were greater at 14 cpm than at 40 cpm in each zone. Amplitude increased from zone 1 to

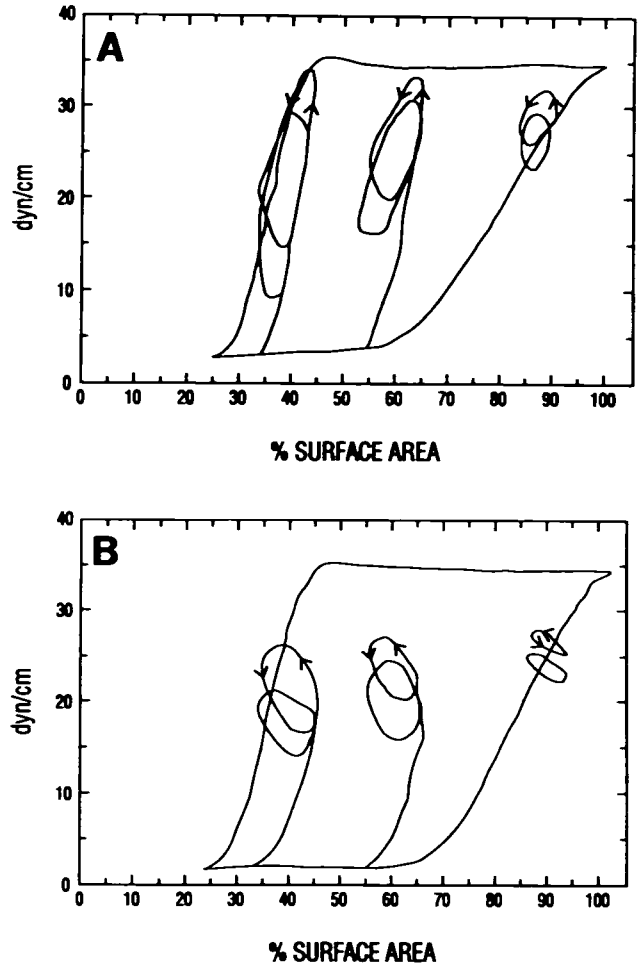

FIGURE 3 Composite of small amplitude surface tension-surface area (γ-A) V_T loops superimposed on standard γ-A diagram. Two loops are shown for each zone; from right to left, zones 1, 2, and 3. The lower loop of each pair is the first V_T loop after simulated V_T breathing was begun from regional A when the lung is at FRC. The second loop of each pair is a representative reproducible loop under steady-state conditions (see text). Compression-decompression cycle frequency was 14 cpm (part A, adult) and 40 cpm (part B, neonate). Each loop rotates counterclockwise (*arrows*).

zone 3; the lowest γ_{min}, 13 and 15 dyn/cm, were recorded in zone 3, and the highest γ_{min}, 26 dyn/cm, in zone 1. All loops rotated counterclockwise.

Direction of the two axes (corrected for the phase lag of the system) of the V_T γ-A loops, i.e., γ_{min} to γ_{max} and A_{min} to

TABLE 3 Surface tensions of open monomolecular films of CLSE

Conditions	Zone 1		Zone 2		Zone 3	
Cycle rate (cpm)	14	40	14	40	14	40
At TLC equivalent	32–35	32–35	32–35	32–35	32–35	32–35
At FRC equivalent	19–24	19–24	<4	<4	<4	<4
V_T γ_{min}	23–26	24–26	18–22	19–21	13–17	15–18
V_T γ_{max}	30–34	27–30	33–34	25–28	34–35	25–29

Surface tension (γ) in dyn/cm of open monolayer films of CLSE in the vertical film surface balance at surface areas (A) equivalent to alveolar A when the lung is at TLC and after compression (expiration) to FRC. Range of γ is given where indicated; <4 dyn/cm was taken as normal low γ for FRC in zones 2 and 3. The range of high γ (γ_{max}) and of low γ (γ_{min}) is given for reproducible V_T γ-A loops that simulate V_T A changes in each zone at cycle rates of 14 cpm (adult) and 40 cpm (neonate) after expiration from TLC to FRC.

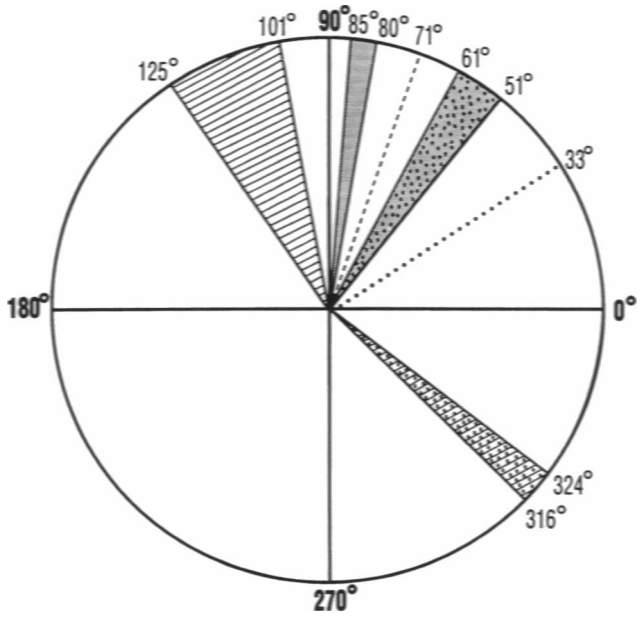

FIGURE 4 Direction (centrifugal) and angle of surface area (A) axes from A_{min} to A_{max} and of surface tension (γ) axes from γ_{min} to γ_{max} of reproducible V_T γ-A loops. At a cycle rate of 14 cpm (first quadrant) there is a phase lag between γ axes (shaded area = range for zones 2 and 3; broken line = average for zone 1) and A axes (stippled shaded area = range for zones 2 and 3; dotted line = average for zone 1). At a cycle rate of 40 cpm, there is a phase shift between γ axes (hashed area = range for zones 1, 2, and 3, second quadrant) and A axes (stippled hashed area = range for zones 1, 2, and 3, fourth quadrant).

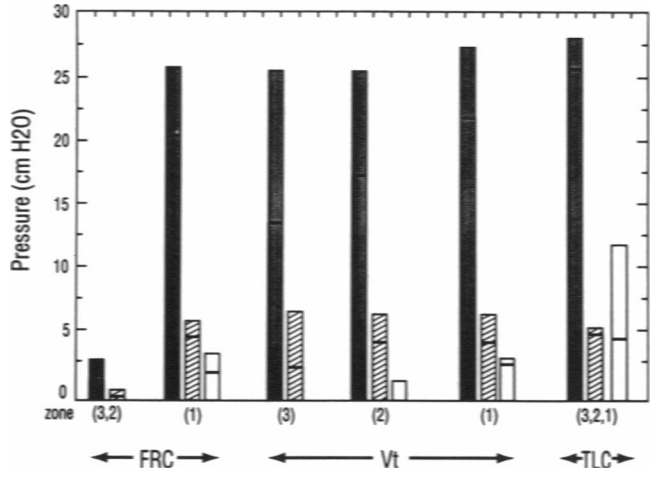

FIGURE 5 Calculated alveolar retractive pressure due to surface tension ($P\gamma$) in the neonate (stippled bars) and in the adult (hashed bars) from data in Table 3, except as noted under FRC (below). Estimated "net" transpulmonary pressure (P_{tp}) from liquid volume-pressure diagrams (top of clear bars) and from alveolar length-tension characteristics (horizontal lines in clear bars) according to data summarized by Hoppin and Hildebrandt (1977). *FRC*: $P\gamma$ calculated from range of γ_{min} in this study, i.e., γ = 3 dyn/cm (top of bars) and γ = 1.5 dyn/cm (horizontal lines) in zones 2 and 3. P_{tp} is 0 in zones 2 and 3. V_T cycles: $P\gamma$ bars shows highest (top) and lowest (horizontal lines) values for highest and lowest γ of superimposable V_T loops; neonatal $P\gamma$ from 40-cpm loops and adult $P\gamma$ from 14-cpm loops. P_{tp} is 0 in zone 3; P_{tp} from length-tension data is 0 in zone 2.

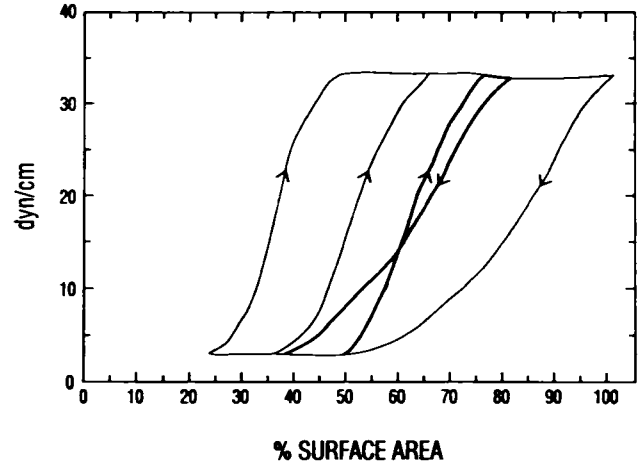

FIGURE 6 Standard surface tension-surface area (γ-A) diagram with superimposed decompression limbs of two successive cycles (*upward arrow*) that start, respectively, at ≈36% A and ≈50% A. The latter, thicker line, in which A expansion is equivalent to inspiration of ≈3 V_T from FRC in zone 2, is followed by compression (thick line) from ≈83% A (*downward arrow*) to the A (≈36% A) at which γ fell to <4 dyn/cm. Crossover in the highlighted cycle shows that A at end-compression (end-expiration) must be less than A at the start of decompression (inspiration) to restore physiological γ_{min} (<4 dyn/cm). Successive large V_T cycles, therefore, would reduce A below the A equivalent to minimal volume after two to three cycles, a physiological contradiction.

A_{max}, is shown in Fig. 4. At 14 cpm, both axes were <90° with the γ axis lagging behind the A axis by ≈27° in zones 2 and 3 and ≈38° in zone 1. At 40 cpm, separation of the two axes widened with the γ axis >90° and the A axis >270° resulting in a phase difference of ≈205° for all zones.

Estimated $P\gamma$ and net P_{tp} values are given in Fig. 5. At FRC, $P\gamma$ > net P_{tp} in all zones at both 14 and 40 cpm; net P_{tp} was 0 in zones 2 and 3. Similarly, $P\gamma$ > net P_{tp} under all conditions of simulated V_T breathing; net P_{tp} was 0 in zone 3. At TLC, $P\gamma$ > net P_{tp} under all conditions with one exception, namely in adult alveoli when liquid P-V data were used for P_{tiss}. In the case of alveolar corners, where radii may be as small as 0.3 μm (Gil et al., 1979), $P\gamma$ at γ = 1.5 dyn/cm would be 98 cm H_2O, and at γ = 35 dyn/cm it would be 2287 cm H_2O.

Additional experiments and related phenomena

In each experiment in which A_{min} was increased from 22% A to 50% A in three consecutive cycles (Fig. 6), γ increased during each decompression from <4 dyn/cm to 32–35 dyn/cm at a mean rate that fell within the range of $d\gamma/dt$ of the standard curves. The A change from γ_{min} to γ_{max} was the same for each decompression curve, 26–30% A, as was the configuration of each curve. Compression from both 100% A and ≈80% A gave similar isotherms in which $d\gamma/dt$ was within the standard range; γ fell to <4 dyn/cm and A decreased 44–46%. One complete cycle is highlighted in Fig. 6 for extrapolation to the condition in vivo. At the start of decompression (inspiration) the film was at 50% A with γ < 4 dyn/cm, and at end-decompression it was at ≈80% A (an increase equivalent to ≈3 V_T) with γ of 33 dyn/cm. Low γ

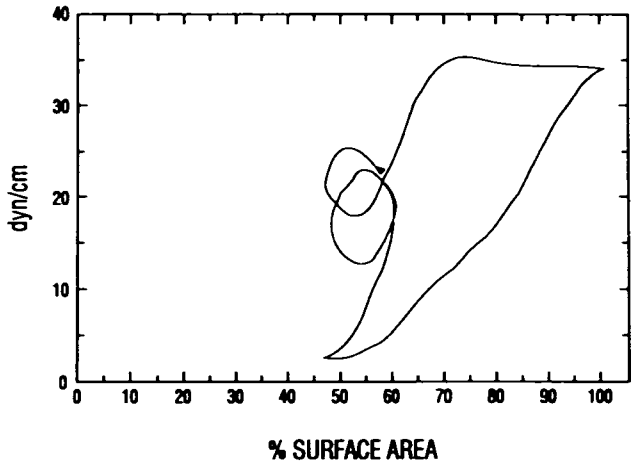

FIGURE 7 Simulation of a "sigh". V_T γ-A loop with arrow after a series (not shown) of superimposable V_T loops at 40 cpm is followed without interruption by decompression (inspiration) to 100% A (TLC), compression (expiration) to ≈46% A (FRC) and resumption of V_T cycling (second V_T loop). Physiological γ (<4 dyn/cm) is fleeting in this maneuver as it is in all other simulations of the predictions of the surface monolayer theory.

was reestablished by compression (expiration) to ≈36% A. Thus, the initial A and final A were not the same: restoration of low γ in the highlighted curves required ≈14% reduction in A, corresponding to a reduction from FRC equivalent to RV equivalent, to reestablish low γ.

The γ-A isotherms during the course of a simulated "sigh" are shown in Fig. 7. During V_T cycling before decompression to 100% A, γ limits were 21 and 27 dyn/cm (zone 2, 40 cpm). Surface tension increased to 34 dyn/cm at 100% A, then decreased to 2 dyn/cm with compression to ≈45% A and rapidly increased to 13 and 23 dyn/cm limits during the succeeding V_T cycle. This pattern is representative of each of 12 trials in four experiments.

Summary

Our findings are summarized in Table 4 with particular regard to the predictions and conditions of the surface monolayer theory.

DISCUSSION

The surface monolayer theory of surfactant function is widely accepted both as originally presented (Clements, 1962; King and Clements, 1972a,b) and as modified in its present form (Goerke and Clements, 1986). However, the presence of a continuous open monolayer at the alveolar surface, in all lung regions and at lung volumes relevant to in vivo conditions, has not been documented; identification of alveolar films in situ, which are virtually always multilayered, is rarely successful (Gil, 1985). The theory rests essentially on information gained from in vitro studies of surface active material (Clements, 1962; King and Clements, 1972a,b; Goerke and Clements, 1986; Notter, 1984), principally in the surface balance, which, however, has not been used to test the theory directly (see Scarpelli (1988) for review). To our knowledge, the present study is the first to simulate in the surface balance the operational requirements of the surface monolayer theory using the model upon which the theory is based (Clements, 1962; Goerke and Clements, 1986).

TABLE 4 Summary of experimental findings with particular regard to the conditions and predictions of the surface monolayer theory (SMT)

Experimental maneuvers/calculations	Experimental findings relevant to the SMT	Are findings compatible with conditions and predictions of the SMT?
Standard γ-A curves (Fig. 2)	Continuous dynamic compression from FRC to V_{min} required to sustain low γ.	NO. SMT predicts sustained low γ at FRC. Compression to V_{min} not possible in vivo.
	Compressed film with high surface pressure tends to move out of container (eg., alveolus).	NO. SMT requires retention of compressed film within alveolus.
V_T cycles from FRC (Fig. 3)	γ always high and unstable during V_T cycles; γ high at FRC in zone 1 and only fleetingly low in zones 2 and 3.	NO. SMT requires stable, low γ at FRC and during V_T breathing. SMT predicts alveolar instability at high γ.
V_T axes (Fig. 4)	Oscillating steady-state rate-dependent high γ.	NO. See preceding comment.
	Phase lag between A and γ at 14 cpm; phase shift at 40 cpm.	NO. SMT predicts concordant A and γ vectors.
	Above findings indicate mixed surface film.	NO. SMT assumes virtually "pure" DPPC film.
$P\gamma$ and net P_{sp} (Fig. 5)	Under virtually all conditions $P\gamma$ exceeds net P_{sp}, which is the condition for alveolar collapse.	NO. SMT predicts stable films of DPPC that resist compression and prevent alveolar collapse. (See also Fig. 2).
Increased V_T cycles (Fig. 6)	Restoration of low γ requires immediate, disproportionate reduction of A during compression phase of V_T cycle.	NO. SMT postulates gradual, relatively small reduction of A to restore/sustain low γ.
The "sigh" (Fig. 7)	Throughout simulated "sigh" (V_T to TLC to FRC to V_T) γ is high and unstable, except for fleeting low γ at FRC.	NO. SMT predicts periodic "sighs" reestablish and sustain stable, low γ.
	γ history is inconsistent with persistent pure DPPC film at any time.	NO. SMT requires persistent "pure" DPPC film between "sighs". (See also Fig. 4).

We chose CLSE as substrate because it is believed to have "normal" surfactant properties in accordance with the monolayer theory (Cummings et al., 1992; Shapiro et al., 1985; Hall et al., 1992; Egan et al., 1984) and, as the commercial preparation Infasurf, has been successfully used as replacement therapy for neonatal respiratory distress syndrome in preterm infants (Yee and Scarpelli, 1991). In a separate series of experiments not reported here, we followed the same protocol as described for CLSE (see Materials and Methods) using surface active material isolated from lung lavage without lipid extraction. We followed conventional preparative methods (King and Clements, 1972a) to obtain an aqueous dispersion of surfactant, including hydrophobic as well as hydrophilic components (phospholipid concentration 10 mg/ml), which was used directly in the surface balance. The results of this study were consistent with the results obtained with CLSE.

We chose our modification of the Langmuir surface balance because there are no measurable leaks in the system (Boyle and Mautone, 1982; Mautone et al., 1988). In support of the surface monolayer theory, it has been suggested that leakage of surface film material onto the walls of the surface balance explains the instability of γ_{min} in vitro (Goerke and Gonzales, 1981; Hildebran et al., 1979). The rates of leakage reported for other surface balances, 0.03–0.05% of the surface material/min, would have had no measurable affect on γ in our study, in which cycle rates were 6, 14, and 40 cpm, and duration of individual experiments was <7 min. In any event, we have found no leaks in our system when using monolayers of pure DPPC (Boyle and Mautone, 1982) or of isolated surface active preparations (Mautone et al., 1988).

The A values for simulated breathing movements were derived from data on relative V in adult lungs in the upright position (Milic-Emili, 1974, 1986) with extrapolation to corresponding alveolar A using morphometric correlations between alveolar V and A (Gil et al., 1979; Mercer et al., 1987). Whereas three regions or zones are distinguishable in the upright adult lung (Hoffman and Heymann, 1990; Milic-Emili, 1974, 1986), these distinctions diminish as height decreases and in the recumbent position where all zones come closer to zone 3 conditions (Hoffman and Heymann, 1990). The broad range of A surveyed in our study encompasses virtually all regions of the lung.

The incompatibility of the surface monolayer theory with normal regional lung function is evident from each experimental approach in our study as summarized in Table 4 and discussed below.

Standard γ-A isotherms

As shown in Fig. 2, reproducible standard γ-A curves with broad A and γ limits is consistent with cyclic reorganization of the surface film between two basically different conformations (Scarpelli, 1968; Scarpelli et al., 1965). Given that γ_{max} (32–35 dyn/cm) exceeds γequil of DPPC ($\approx$25 dyn/cm), it is reasonable to assume that the expanded film contains DPPC plus mixed material adsorbed from the hypophase, and given that γ falls to near 0 during compression, it is also reasonable that non-DPPC components are "squeezed out" (Goerke and Gonzales, 1981) of the surface to leave a DPPC-rich film that collapses (bend in the compression curve) at the same relative A as films of pure DPPC (Colacicco and Scarpelli, 1973). These are fundamental assumptions of the surface monolayer theory. However, extrapolation from standard curves to lung function in vivo mitigates against the theory: First, the A limits are equivalent to unattainable breathing movements between TLC and V_{min}. Second, γ_{max} is high and incompatible with normal liquid transfers and structural stability at the alveolar level (Pattle, 1955, 1958; Scarpelli, 1971). Third, maintenance of a steady physiological γ_{min} requires continuous compression; γ_{min} increases rapidly when compression is reversed and also when A is held constant (Scarpelli and Mautone, 1994), i.e., γ may be expected to increase rapidly during both inspiration and at end-expiration. Fourth, film surface pressure at all γ values and particularly at γ_{min}, where it is highest, would promote movement of monolayer material in the direction shown by the small arrows in Fig. 1, i.e., out of alveoli, because surfactants in open films move from loci of high surface pressure (low γ) to loci of low surface pressure (high γ) until surfactant distribution is uniform at γequil throughout the film (the Marangoni effect) (Scarpelli, 1968). Even if surfactant movement were restricted or arrested in situ by the large reduction of A from alveoli to airways, γ of the open film would equilibrate rapidly at the unphysiologically high γequil of surfactants, $\approx$25–30 dyn/cm. It is relevant to note here that this problem is virtually eliminated in closed (bubble) films (Scarpelli et al., 1965; Colacicco and Scarpelli, 1973; Scarpelli, 1988).

Simulated regional breathing

Our study indicates (Fig. 3) that γ of the open monolayer is always high at TLC in all zones; that differential reduction of A among regions during expiration from TLC to FRC would lower alveolar γ transiently to <4 dyn/cm in zones 2 and 3, and to 19–24 dyn/cm in zone 1; that γ would increase immediately as V_T breathing is resumed; and that γ fluctuates between limits of high γ when a steady state is rapidly achieved during V_T breathing in all zones. These characteristics contradict each requirement of the surface monolayer theory as follows: Low, near 0 γ is produced only briefly in two of the three zones and not at all in the third; sustained or stable low γ cannot be expected because its precondition, continuous compression of the open film, is an artifact of laboratory manipulation, in contrast with the A expansion that occurs when V_T breathing follows expiration to FRC in vivo (Milic-Emili, 1974, 1986); and high γ, which is three to eight times higher than the "stable" γ predicted in the theory, is variable but steady in all zones at both 14 and 40 cpm as long as V_T cycling is continued. In summary, the low γ required by the theory is fleeting and unstable, whereas

unphysiologically high γ is sustained in all regions under the operational conditions of the theory.

V_T γ-A LOOPS

Our study shows (Fig. 4) that relatively low-amplitude cycling of the open monolayer at adult and neonatal V_T frequencies yields γ significantly higher than the near 0 γ predicted by the theory. The γ range, in which γ_{max} exceeds γequil of pure DPPC (Goerke and Clements, 1986; Notter, 1984; Colocicco and Scarpelli, 1973), suggests that the monolayer is a mixed film, i.e., that a pure film of DPPC is not sustained during V_T cycling in all zones. This aspect of surfactant function in vivo, which occupies most of the time spent breathing, is not addressed in the surface monolayer theory.

The phase lag between A and γ axes at 14 cpm shows that the γ changes induced by V_T compression and decompression, respectively, lag behind the A changes. The reasons for this apparent inertia, which results in a counterclockwise rotation of the loop, cannot be defined by our study. Fundamental processes that may be considered include adsorption and desorption kinetics between the surface and hypophase, water shifts at these sites, lateral movement of molecules in the plane of the surface, and changing orientation of the molecules normal to the surface (Scarpelli, 1968; Colocicco and Scarpelli, 1973; Notter, 1984; Mautone et al., 1988). Collectively, these processes can be assessed in terms of surface elasticity and viscosity (Prinz and van den Tempel, 1969; Mautone et al., 1988). The phase shift when rate is increased to 40 cpm suggests that surface inertial and viscoelastic factors have established a second-order system in response to rapid oscillation of applied force. Although additional study is required, it is clear that the low-amplitude, high-frequency excursions of simulated V_T breathing produce an oscillating steady-state rate-dependent high γ that is inconsistent with the surface monolayer theory.

Net P_{tp} and $P\gamma$

Estimates of net P_{tp} lead to equivocal interpretation only in the case of adult alveoli at TLC, where $P\gamma$ < net P_{tp} using liquid P-V data and $P\gamma$ > net P_{tp} using tissue tension data (Fig. 5). Given that liquid and tissue-derived P-V curves are disparate only >80% V (90% A), the discrepancy has limited functional significance. On the other hand, our study shows that $P\gamma$ was >net P_{tp} under all other conditions of the surface monolayer theory, including FRC and V_T breathing at adult and neonatal frequencies, and TLC at neonatal frequency. In the open monolayer (Fig. 1), $P\gamma$ > net P_{tp} would establish conditions for alveolar collapse and/or alveolar edema formation (Pattle, 1955, 1958; Clements, 1962). Where P_{tp} is 0, a sustained γ of 0 is required but not effected in the open monolayer. Thus, under virtually all conditions of lung function, γ in monolayers operating in accordance with the theory is not consistent with stability of air-inflated alveoli. In addition, the $P\gamma$ that would be generated in alveolar corners is extraordinary: ≈100 to >2000 cm H_2O.

Variation of A limits

As long as γ limits were 32–35 dyn/cm and <4 dyn/cm the respective slopes of compression and decompression isotherms did not change as A limits were decreased, indicating that film transformations as described under Standard γ-A Isotherms were also unchanged (Fig. 6). Given that $d\gamma/dt$ was higher during decompression than during compression, A expansion had to exceed A reduction by ≈14% to prevent crossover of the two curves in any given cycle. The isotherms indicated by thick lines in Fig. 6 illustrate the problem. After decompression from ≈50% A (FRC) to ≈80% A (equivalent to an inspiration of ≈3 V_T), γ_{min} was restored only after A reduction (expiration) to 36% A (RV). Although monolayer film dynamics in this case are in accord with the surface monolayer theory, they are incompatible with normal lung function for the following reasons: First, the inspiratory-expiratory ratio in vivo would become a fundamental determinant of alveolar γ during each respiratory cycle. Shortened expirations would not lower γ to the required γ_{min}, whereas restoration of γ_{min} would require A reduction greater than the preceding A expansion. Second, in the latter case, lung V would be reduced below V_{min} in a few breaths. Third, the A dependence of γ does not permit stable low γ as required by the theory. As shown in Fig. 6, γ varies at any given A depending on the immediate γ-A history of the film, in contrast with the demonstrated uniformity of γ among alveoli of different A (Schurch, 1982). Fourth, to the extent that inspiratory time might be extended to avoid the crossover problem, the duration of high alveolar γ would be extended simultaneously.

Simulated "sigh"

According to the surface monolayer theory, a DPPC-rich film and stable low γ are reestablished periodically by inspiration to TLC followed by resumption of V_T breathing from FRC. Simulation of this maneuver produced low γ after compression from 100% A (TLC) to 45%-50% A (FRC) (Fig. 7). If the DPPC-rich film had been reestablished, its existence was fleeting, because for virtually the entire period of this exercise γ was high and unstable. Calculated $P\gamma$ was greater than net P_{tp}.

Another study has used a new experimental approach in an attempt to validate the monolayer theory (Schurch et al., 1989) in which surface films are spread at the air-liquid interface of a gas pocket entrapped in bulk liquid, the "captive bubble" technique. Basically, a bubble is formed in liquid; the surface is closed. Under these conditions, when A is reduced by applying very high pressure to the system, near 0 γ can be sustained for minutes. Paradoxically, this in vitro model is not the analogue of an open film; rather, it is a closed film, which supports the original observations of Pattle (1955, 1958) that surfactant sustains near 0 γ in bubble films and our observations (Scarpelli, 1978; Scarpelli et al., 1984) that intraalveolar surfactant bubbles, which are formed naturally in vivo, also sustain near 0 γ.

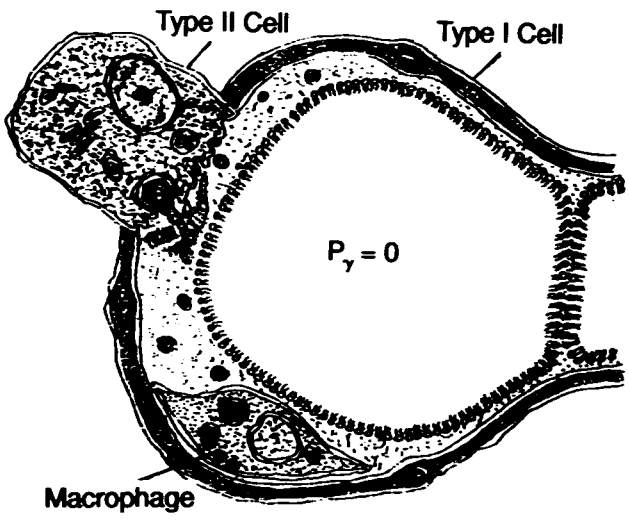

FIGURE 8 Our modification of the model of the surface monolayer theory of Fig. 1. It is based on previous reports of intraalveolar bubble film formation in vivo and in excised lungs (see text). The closed bubble film differs from the open monolayer as follows. It is self-contained; the surfactant molecules ( ) are closer to each other, i.e., they are compressed spontaneously to produced stable, virtually 0 γ; virtually 0 γ lowers retractive pressure caused by γ ($P\gamma$) to virtually 0 (the collapsing force shown by broad arrows in Fig. 1 is eliminated); the bubble films may be a monolayer over the hypophase that covers epithelial cells and macrophages, and it is a bilayer or "foam film" where it apposes the gas phase; the closed film arrests the movement of surfactant molecules out of alveoli (thin arrows in Fig. 1) and provides infrastructural support against alveolar collapse.

Bubble films

We generated bubbles (50–1600 μm diameter) by agitating aerated bulk CLSE on a vortex mixer. We used the criteria of Pattle (1955, 1958) to compare CLSE bubble films with bubble films formed naturally in vivo (Scarpelli, 1978, 1988; Scarpelli et al., 1979; 1984; Mautone et al., 1992). We found that CLSE films, like natural intraalveolar bubble films, produce spontaneously near 0 γ; that near 0 γ and film structure are stable for hours; and that the films are highly permeable to respiratory gases. Based on the topography of bubbles and bubble films in situ, as observed and photographed by stereomicroscopy (in the studies cited above) and on the known configuration of bubble films at bubble/liquid and bubble/bubble interfaces (Bikerman, 1973), we suggest that the film configuration shown in Fig. 8 is consistent with surfactant film structure and function in situ.

This work was supported by National Heart, Lung and Blood Institute grant HL-38303.

REFERENCES

Bikerman, J. J. 1973. Foams. Springer-Verlag, New York.

Bligh, E., and W. Dyer. 1959. A rapid method of total lipid extraction and purification. *Can. J. Biochem.* 37:911–917.

Boyle, J., and A. J. Mautone. 1982. A new surface balance for dynamic surface tension studies. *Colloids Surf.* 4:77–85.

Clements, J. A. 1962. Surface phenomena in relation to pulmonary function. *Physiologist.* 5:11–28.

Colacicco, G., and E. M. Scarpelli. 1973. Pulmonary surfactants: molecular structure and biological activity. *In* Horizons in Surface Science. L. M. Prince and D. F. Sears, editors. Academic Press, New York.

Cummings, J. J., B. A. Holm, M. L. Hudak, B. B. Hudak, W. H. Ferguson, and E. A. Egan. 1992. A controlled clinical comparison of four different surfactant preparations in surfactant-deficient preterm lambs. *Amer. Rev. Resp. Dis.* 145:999–1004.

Egan, E. A., R. H. Notter, M. S. Kwong, and D. L. Shapiro. 1984. Natural and artificial lung surfactant replacement therapy in premature lambs. *J. Appl. Physiol.* 55:875–883.

Engel, S. 1962. Lung Structure. Charles C Thomas, Springfield, IL.

Gil, J. 1985. Histological preservation and ultrastructure of alveolar surfactant. *Ann. Rev. Physiol.* 47:753–763.

Gil, J., H. Bachofen, P. Gehr, and E. R. Weibel. 1979. Alveolar volume-surface area relation in air- and saline-filled lungs fixed by vascular perfusion. *J. Appl. Physiol.* 47:990–1001.

Goerke, J., and J. A. Clements. 1986. Alveolar surface tension and lung surfactant. *In*: Handbook of Physiology, Section 3: The Respiratory System, Vol III: Mechanics of Breathing (Part 1), P. T. Macklem and J. Mead, editors. American Physiological Society, Bethesda, Maryland.

Goerke, J., and J. Gonzales. 1981. Temperature dependence of dipalmitoylphosphatdylcholine monolayer stability. *J. Appl. Physiol.* 51:1108–1114.

Hall, S. B., A. R. Venkitraman, J. Whitsett, B. A. Holm, and R. Notter. 1992. Importance of hydrophobic apoproteins as constituents of clinical exogenous surfactants. *Am. Rev. Respir. Dis.* 145:24–30.

Hawgood, S., and J. A. Clements. 1990. Pulmonary surfactant and its apoproteins. *J. Clin. Invest.* 86:1–6.

Hildebran J. N., J. Goerke, and J. Clements. 1979. Pulmonary surface film stability and composition. *J. Appl. Physiol.* 47:604–611.

Hoffman, J. E., and M. A. Heymann. 1990. Pulmonary circulation. *In* Pulmonary Physiology: Fetus Newborn Child Adolescent. E. M. Scarpelli, editor. Lea and Febiger, Philadelphia.

Hoppin, F. G., and J. Hildebrandt. 1977. Mechanical properties of the lung. *In* Lung Biology in Health and Disease, C. Lenfant, editor. Vol. 3: Bioengineering Aspects of the Lung, J. West, editor. Marcel Dekker, Inc. New York.

King, R. J., and J. A. Clements. 1972a. Surface active material from dog lung II. Composition and physiological correlations. *Amer. J. Physiol.* 223: 715–726.

King, R. J., and J. A. Clements. 1972b. Surface active material from dog lung III. Thermal analysis. *Amer. J. Physiol.* 223:727–733.

Mautone A. J., M. T. Antonio-Santiago, B. C. Clutario, and E. M. Scarpelli. 1992. Temperature affects mechanics and stability during initial inflation-deflation of mature fetal lung. *Pediatr. Pulmonol.* 13:203–208.

Mautone, A. J., A. Ritter, and J. Boyle. 1988. A new method to evaluate expansion-compression stress-strain properties of surface films of biological surfactants. *Colloids Surf.* 300:223–241.

Mercer, R. R., J. M. Laco, and J. D. Crapo. 1987. Three-dimensional reconstruction of alveoli in the rat lung for pressure-volume relationships. *J. Appl. Physiol.* 62:1480–1487.

Milic-Emili, J. 1974. Pulmonary statics. *In* Respiration Physiology, Vol. 1. J. Widdicombe, editor. University Park Press, Baltimore.

Milic-Emili, J. 1986. Static distribution of lung volumes. *In* The Handbook of Physiology, Section 3: The Respiratory System; Vol. III, Mechanics of Breathing, Part 2. P. Macklem, and J. Mead, editors. The American Physiological Society, Bethesda, MD.

Notter RH 1984. Surface chemistry of pulmonary surfactant: the role of individual components. *In* Pulmonary Surfactant. B. Robertson, L. M. G. Van Golde, J. J. Batenburg, editors. Elsevier, Amsterdam.

Pattle, R. E. 1955. Properties, function and origin of the alveolar lining layer. *Nature.* 175:1125–1126.

Pattle, R. E. 1958. Properties, function, and origin of the alveolar lining layer. *Proc. Royal Soc. (Lond.) B Biol. Sci.* 148:217–240.

Prinz, A., and van den Tempel, M. 1969. Composition and elasticity of thin liquid films. *J. Physic. Chem.* 73:2828–2834.

Scarpelli, E. M. 1968. The Surfactant System of the Lung. Lea and Febiger, Philadelphia. 9–29, 101–144.

Scarpelli, E. M. 1971. Physiology and pathology of pulmonary surfactants. *Triangle.* 10:47–56.

Scarpelli, E. M. 1978. Intrapulmonary foam at birth: an adaptational phenomenon. *Pediat. Res.* 12:1070–1076.

Scarpelli, E. M. 1988. Surfactants and the Lining of the Lung. The Johns Hopkins University Press, Baltimore.

Scarpelli, E. M., B. C. Clutario, A. J. Mautone, and J. Baum. 1984. Intrasaccular bubbles of near-zero surface tension stabilize neonatal lungs. *Pfluegers Archiv. Eur. J. Physiol.* 401:287–292.

Scarpelli, E. M., B. C. Clutario, and D. Traver. 1979. Failure of immature lungs to produce foam and retain air at birth. *Pediat. Res.* 13:1285–1292.

Scarpelli, E. M., K. H. Gabbay, and J. A. Kochen. 1965. Lung surfactants, counter-ions and hysteresis. *Science.* 148:1607–1609.

Scarpelli, E. M., and A. J. Mautone. 1994. The surface monolayer theory does not explain surfactant function in vivo. *Pediatr. Pulmonol.* In press.

Schurch, S. 1982. Surface tension at low lung volumes: dependence on time and alveolar size. *Respir. Physiol.* 48:339–355.

Schurch, S, H. Bachofen, J. Goerke, and F. Possmeyer. 1989. A captive bubble method reproduces the in situ behavior of lung surfactant monolayers. *J. Appl. Physiol.* 67:2389–2396.

Shapiro, D. L., R. H. Notter, F. C. Morin, K. S. Deluga, L. M. Golub, R. A. Sinkin, K. I. Weiss, and C. Cox. 1985. Double-blind, randomized clinical trial of a calf lung extract administered at birth to very premature infants for prevention of respiratory distress syndrome. *Pediatrics* 76: 593–599.

Weibel, E. R. 1963. Morphometry of the Human Lung. Springer-Verlag, Heidelberg.

Yee, W. H., and E. M. Scarpelli. 1991. Surfactant replacement therapy. *Pediatr. Pulmonol.* 11:65–76.